

A HIGH-ORDER HARMONIC BALANCE METHOD FOR SYSTEMS WITH DISTINCT STATES

Malte Krack^{1,*}, Lars Panning-von Scheidt¹, Jörg Wallaschek¹

Abstract

A pure frequency domain method for the computation of periodic solutions of nonlinear ordinary differential equations (ODEs) is proposed in this study. The method is particularly suitable for the analysis of systems that feature distinct states, i. e. where the ODEs involve piecewise defined functions. An event-driven scheme is used which is based on the direct calculation of the state transition time instants between these states. An analytical formulation of the governing nonlinear algebraic system of equations is developed for the case of piecewise polynomial systems. Moreover, it is shown that derivatives of the solution of up to second order can be calculated analytically, making the method especially attractive for design studies.

The methodology is applied to several structural dynamical systems with conservative and dissipative nonlinearities in externally excited and autonomous configurations. Great performance and robustness of the proposed procedure was ascertained.

Keywords: harmonic balance method, nonlinear oscillations, systems with distinct states, periodic solutions to nonlinear ordinary differential equations, event-driven scheme

*Corresponding author

Email address: krack@ila.uni-stuttgart.de (Malte Krack)

1. Introduction

In the fields of science and engineering, a common task is the calculation of periodic solutions of nonlinear ordinary differential equations. In our study, we will focus on ODEs of arbitrary dimension involving generic, i. e. possibly strong and non-smooth nonlinear functions. In particular, we will address systems that can comprise distinct states so that the nonlinear functions are only piecewise defined. In mechanical engineering, such nonlinearities arise e. g. in structural systems with contact joints, where stick, slip and lift-off are often considered as locally distinct states [1]. In electrical engineering, examples for such systems are electrical circuits, where e. g. transistors, rectifiers and switches induce distinct system states. A rheological example are superelastic shape memory alloys where the phases and phase transformations between e. g. martensite and austenite phase can be regarded as distinct states [2]. Of course, many other examples can be found in various fields of science and engineering.

In order to find periodic solutions to such problems, analytical approaches are often not applicable and computational methods have to be employed. Besides the family of time integration methods, so called frequency domain methods are commonly used due to their often superior computational efficiency. The basic idea of frequency domain methods is to choose a truncated Fourier ansatz for the dynamic variables, thereby exploiting the periodic nature of the solution. This class of methods gives rise to nonlinear algebraic systems of equations. Depending on whether the solution is sought in the frequency domain or in a collocated time domain, and whether the residual is formulated in the frequency or time domain, the methods can be grouped into (Multi-)Harmonic Balance Method [3, 4], Trigonometric Collocation Method [5] and Time Spectral Method [6]. Among these methods, the Multi- or High-order Harmonic Balance Method (HBM) is probably the most commonly applied method.

For the HBM, it is generally necessary to compute the spectrum of the nonlinear function that governs the ODE. This task can generally be performed by different methods. In the following, we will focus on those methods that are

capable of treating systems with distinct states.

The Alternating-Frequency-Time (AFT) scheme [7] is one of the most commonly applied approaches in this context. The AFT scheme involves a sampling of the nonlinear function and subsequent back-transformation into frequency domain. Advantages of this method are the broad applicability, the comparatively small implementation effort and the low computational effort for evaluating the residual function. The latter aspect is particularly true if the (Inverse) Fast Fourier Transform is used for the transformation between time and frequency domain. A drawback is that nonlinearities with distinct states involve special treatment. A sampling of the nonlinear function is not straight-forward, because the current state at a specific time instant is not always a priori known. So called predictor-corrector schemes [8] are frequently employed to perform the switching between different states for these systems. In classical AFT schemes, the sampling points are fixed, and do not need to coincide with the state transition time instants. This inherently induces discretization errors. Hence, the sensitivity of the transition time instants with respect to arbitrary parameters cannot be captured accurately, resulting in inaccurate derivatives, in particular for higher order derivatives.

More recently, a purely frequency-based formulation was proposed by COCHELIN AND VERGEZ [9]. The authors applied the Asymptotic Numerical Method to expand the periodic solution into a power series based on high-order derivatives of the nonlinear function. In order to obtain these derivatives efficiently, a so called quadratic recast is performed where the original system of equations is transformed into a system of only quadratic order. An advantage of this method is the computationally robust and efficient continuation of the solution. A drawback is obviously the required quadratic recast which can be difficult for generic types of nonlinear functions. Moreover, systems with distinct states need to be artificially smoothed in order to accomplish a closed-form quadratic recast. This smoothing procedure induces inaccuracies compared to the original non-smooth model.

In order to avoid the shortcomings of a required recast or the degenerated ac-

curacy due to sampling, a pure frequency domain formulation for the original system with distinct states can instead be used. Such an approach necessarily involves the direct calculation of the transition time instants between the states. For high-order HBM, these approaches have only been developed for special types of nonlinearities so far. For example PETROV AND EWINS [10] developed an analytical formulation of the HBM for piecewise linear friction interface elements in structural dynamical problems. In this study, the approach in [10] is extended to generic systems with an arbitrary number of distinct states, see Section 2. Analytical formulations can be developed in case of piecewise polynomial systems, as it will be shown in Subsection 2.5. Moreover, the formulation facilitates the analytical calculation of gradients of up to second order as an inexpensive postprocessing step, see Subsection 2.4. To demonstrate the capabilities and the performance of the proposed methodology, several numerical examples are studied in Section 3. Finally, conclusions are drawn in Section 4.

2. Methods of Analysis

2.1. Harmonic Balance Method for systems with distinct states

Consider a system whose dynamics can be described by a first-order ordinary differential equation,

$$\dot{\mathbf{y}} = \mathbf{f}(\mathbf{y}, t) , \tag{1}$$

in which $\dot{(\)}$ denotes derivative with respect to time t . It is assumed that the generally nonlinear function \mathbf{f} is piecewise defined within closed regions of the state space of \mathbf{y} . These closed regions in state space are denoted *states* throughout this paper. These states shall not be confused with the vector \mathbf{y} which is sometimes also referred to as state in literature since it represents a point in state space.

As time evolves, the system can assume several states, see Fig. 1. A transition between these states is termed state transition and the corresponding time instant is called state transition time instant in the following. The system enters a specific state at the corresponding transition time t^- and leaves it at t^+ .

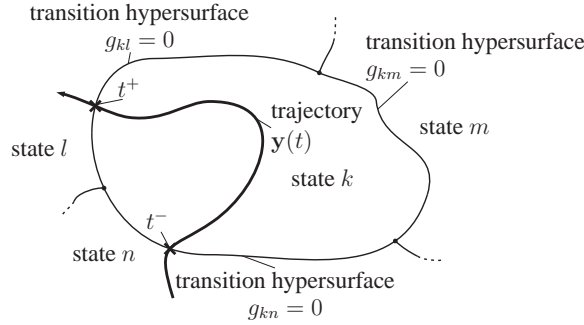


Figure 1: Illustration of the dynamics of a system with distinct states

Each possible state k consists of a nonlinear function \mathbf{f}_k , transition conditions g_{kl} which roots define a transition hypersurface to state l , and internal variables \mathbf{v}_k :

Definition of ‘state k ’

Nonlinear function: $\mathbf{f}_k(\mathbf{y}(t), \mathbf{v}_k, t)$,

Transition conditions: $g_{kl}(\mathbf{y}(t), \mathbf{v}_k, t)$, $\forall l \in \mathcal{L}_k$,

Internal variables: $\mathbf{v}_k(\mathbf{y}(t^-), \mathbf{f}(t^-))$. (2)

The set \mathcal{L}_k is a set of integers indicating a possible next state, the system can assume after being in state k .

It is assumed that the function \mathbf{f} is smooth within a state and continuous at the state transitions. It should be noted at this point that the advantages of the proposed method can be particularly exploited for the case of piecewise polynomial systems, as it will be shown in Subsection 2.5, although the derivations in the following are not restricted to these.

Internal variables are introduced in the state definition (2) to facilitate the treatment of hysteresis effects. In a hysteretic system, the dynamics do not explicitly depend on the current value $\mathbf{y}(t)$ but on the time history of \mathbf{y} . Internal variables can therefore be used to carry this history-dependent effect over the state hypersurface, which manifests itself in the dependence of the nonlinear function \mathbf{f}_k and the transition hypersurface g_{kl} on \mathbf{v}_k , see Eq. (2). Note that hysteretic

systems will also be addressed in the numerical examples. For systems without these effects, of course, the introduction of internal variables is not necessary. Periodic, steady-state solutions to Eq. (1) are sought in this study. To this end, the High-order Harmonic Balance Method can be applied [4]. Hence, a Fourier series truncated to harmonic order H represents the ansatz for the dynamic variables $\mathbf{y}(t)$,

$$\mathbf{y}(t) \approx \sum_{n=-H}^H \mathbf{Y}_n e^{in\Omega t} \quad (3)$$

Herein, Ω is the fundamental angular frequency of the response and $i = \sqrt{-1}$ is the imaginary unit. The Fourier coefficients \mathbf{Y}_n are symmetric, $\mathbf{Y}_{-n} = \overline{\mathbf{Y}_n}$, where $\overline{(\)}$ denotes complex conjugate, since $\mathbf{y}(t)$ is a real-valued function in time. Substitution of Eq. (3) into the differential equation (1) and Fourier-Galerkin projection [3] gives rise to a nonlinear algebraic system of equations in the unknowns \mathbf{Y}_n and τ_j^-, τ_j^+ ,

$$\text{solve } in\Omega \mathbf{Y}_n - \mathbf{F}_n(\mathbf{Y}_{-H}, \dots, \mathbf{Y}_H) = \mathbf{0}, \quad n = -H, \dots, H, \quad (4)$$

$$\text{with } \mathbf{F}_n = \frac{1}{2\pi} \int_{(2\pi)} \mathbf{f}(\mathbf{y}, \tau) e^{-in\tau} d\tau = \frac{1}{2\pi} \sum_{j=1}^J \int_{\tau_j^-}^{\tau_j^+} \mathbf{f}(\mathbf{y}, \tau) e^{-in\tau} d\tau, \quad (5)$$

$$\text{subject to } \tau_J^+ = \tau_1^- + 2\pi, \quad \tau_j^+ = \tau_{j+1}^- \quad \forall j = 1 \dots J. \quad (6)$$

For convenience, the normalized time $\tau = \Omega t$ has been introduced. During one period of oscillation, the system assumes a total number of J states. It should be emphasized that neither the set of states nor the state transition time instants τ_j^-, τ_j^+ are a priori known. As indicated in the constraint Eq. (6), the τ_j^-, τ_j^+ are periodic and continuous to cover an entire time period, as a consequence of the periodic ansatz. In this study, it is proposed to directly compute the periodic set of transition time instants τ_j^-, τ_j^+ , which is developed in the following subsection.

Once the transition time instants are known for given \mathbf{Y}_n , the integrals in Eq. (5) can be evaluated to formulate the residual in Eq. (4). Owing to the piecewise definition of the function \mathbf{f} , it is convenient to split up the integral in Eq. (5) into J summands, where each of the summands is an integral with the transition

time instants as integral limits.

2.2. Periodic set of state transition time instants

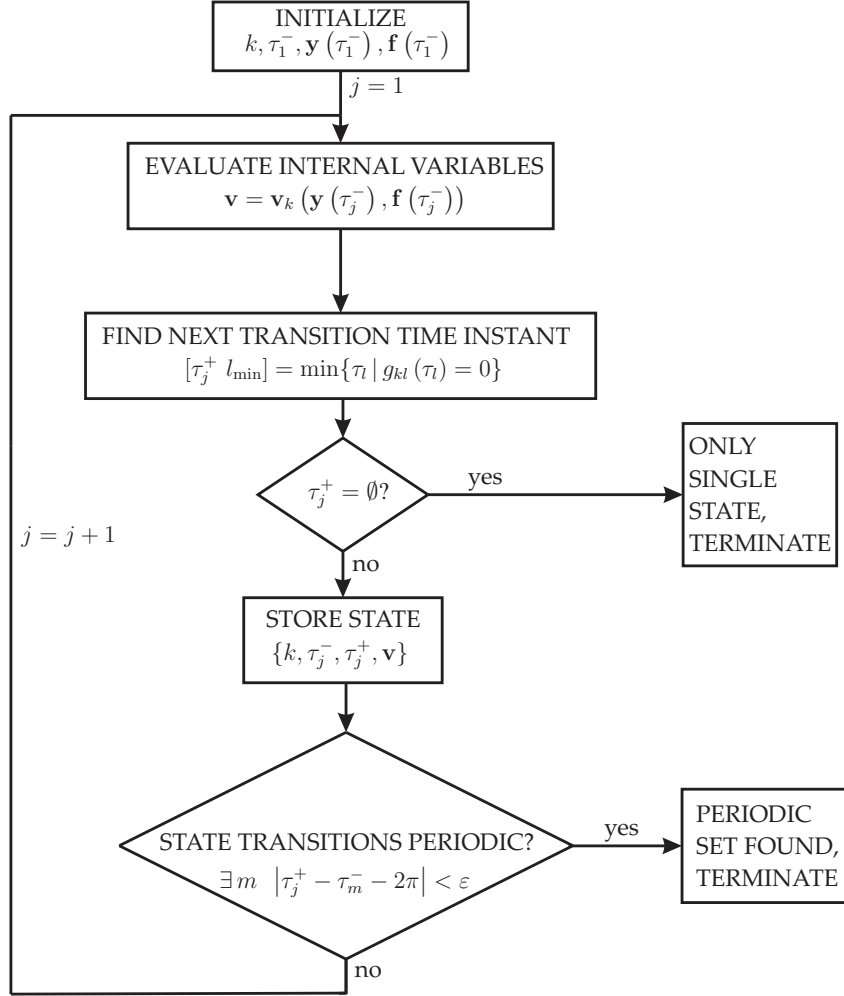


Figure 2: Algorithm for the calculation of the periodic set of state transition time instants

In Fig. 2, an algorithm is summarized that is capable of finding a periodic set of state transition time instants for an arbitrary system with or without distinct states. Starting from an initial time τ_1^- , state k and according initial function value $\mathbf{f}(\tau_1^-)$, the next states are iteratively computed until a periodic set of

state transitions is found. It is therefore assumed that a periodic set of state transitions exists and the algorithm is attracted to it. During the numerical studies, no case was observed where this assumption was disproved.

After evaluating the internal variables, the next roots τ_l of all possible state transition conditions g_{kl} are computed and the minimum is taken. In the special case when there is no next state, the system remains in this state for all times and the algorithm terminates. Note that this includes the special class of systems with only a single state.

If a next state exists, the current state is stored for subsequent evaluation of the Fourier coefficients. If the state transitions are periodic - according to a specified tolerance ε - the algorithm can terminate, otherwise j is incremented and the loop is repeated.

2.3. Computation and continuation of the solution

In general, the solution to Eqs. (4)-(6) cannot be obtained in closed form and an iterative numerical procedure has to be employed instead. In this study, a Newton-Raphson method combined with a predictor-corrector continuation scheme was used [11]. The numerical performance of the solution procedure was greatly enhanced by providing analytically calculated gradients of the residual, as derived in the following subsection.

2.4. Analytical calculation of gradients and sensitivities of the solution

Gradients of the residual are often required in a numerical solution procedure for the algebraic system of equations in Eq. (4). Moreover, higher-order derivatives at the solution point can be used to expand the solution in a Taylor series. An approximate solution thus becomes available in the vicinity of the current solution point in parameter space without the need for re-computation. The Taylor expansion with respect to the unknown variables can be employed as a predictor in a numerical continuation procedure. Taylor expansions with respect to system parameters are particularly interesting for parametric studies, uncertainty analysis and optimization.

In this study, the analytical calculation of gradients of first and second order is presented. We focus on the Fourier coefficients of the nonlinear function \mathbf{f} since the sensitivities of the other term in Eq. (4) is straight-forward. The first and second order sensitivities of \mathbf{F}_n read

$$\frac{\partial \mathbf{F}_n}{\partial \psi} = \sum_{j=1}^J \int_{\tau_j^-}^{\tau_j^+} \frac{\partial \mathbf{f}}{\partial \psi} e^{-in\tau} d\tau + \mathbf{f}(\tau_j^+) \frac{\partial \tau_j^+}{\partial \psi} - \mathbf{f}(\tau_j^-) \frac{\partial \tau_j^-}{\partial \psi} = \sum_{j=1}^J \int_{\tau_j^-}^{\tau_j^+} \frac{\partial \mathbf{f}}{\partial \psi} e^{-in\tau} d\tau, \quad (7)$$

$$\frac{\partial^2 \mathbf{F}_n}{\partial \phi \partial \psi} = \sum_{j=1}^J \int_{\tau_j^-}^{\tau_j^+} \frac{\partial^2 \mathbf{f}}{\partial \phi \partial \psi} e^{-in\tau} d\tau + \frac{\partial \mathbf{f}(\tau_j^+)}{\partial \psi} \frac{\partial \tau_j^+}{\partial \phi} - \frac{\partial \mathbf{f}(\tau_j^-)}{\partial \psi} \frac{\partial \tau_j^-}{\partial \phi}. \quad (8)$$

Herein, ϕ, ψ are arbitrary scalar variables such as the components of the Fourier coefficients \mathbf{Y}_n , the frequency Ω or any system parameter. The Leibniz integral rule was applied to derive Eqs. (7) and (8) since the integral limits might and often do depend on the parameters. Note that the last two summands in the first-order sensitivity cancel each other out in the sum over one period due to the assumed continuity of \mathbf{f} and the periodicity condition in Eq. (6).

The calculation of the derivative of the function \mathbf{f} within a state is typically straight-forward. In contrast, the sensitivities of a transition time instant τ_j is more complex. It has to be calculated by implicit differentiation of the active transition condition $g(\tau_j) = 0$. The resulting first- and second-order sensitivities of the transition time instants read

$$\begin{aligned} \frac{\partial \tau_j}{\partial \psi} &= \left[\frac{\partial g}{\partial \tau} \right]^{-1} \frac{\partial g}{\partial \psi}, \\ \frac{\partial^2 \tau_j}{\partial \phi \partial \psi} &= \left[\frac{\partial g}{\partial \tau} \right]^{-1} \left[\frac{\partial^2 g}{\partial \phi \partial \psi} + \frac{\partial g}{\partial \phi} \frac{\partial \tau_j}{\partial \psi} + \frac{\partial g}{\partial \psi} \frac{\partial \tau_j}{\partial \phi} \frac{\partial^2 g}{\partial \tau^2} \frac{\partial \tau_j}{\partial \phi} \frac{\partial \tau_j}{\partial \psi} \right]. \end{aligned} \quad (9)$$

In Eq. (9), all functions are evaluated at the transition time instant τ_j . It should be remarked that the time derivative of the transition condition $\frac{\partial g}{\partial \tau}$ is nonzero at a regular zero crossing so that the inverse in Eq. (9) is well-defined. Note that only first-order derivatives of the state transition time instants τ_j are directly included in Eq. (8). However, second-order derivatives may be required for the calculation of the sensitivities of the internal variables $\mathbf{v}_k(\mathbf{y}(\tau_j^-), \mathbf{f}(\tau_j^-))$, see definition (2).

2.5. Application to piecewise polynomial systems

All previous developments are valid for the class of piecewise smooth systems. In the sequel of this study, we will focus on the large subclass of piecewise polynomial systems. For this class, all functions $\mathbf{f}_k, g_{kl}, \mathbf{v}_k$ are polynomials in the components of \mathbf{y} , which makes the efficient formulation of the previously derived expressions particularly cheap. In order to solve Eqs. (4)-(6) the basic operations (a) *add/subtract*, (b) *multiply*, (c) *integrate* and (d) *calculate roots* are required to find the periodic set of state transitions and to carry out the integration indicated in Eq. (5). These operations can be directly performed in Fourier space.

The *multiplication* of two scalar functions $a(\tau), b(\tau)$ with associated Fourier coefficients $\mathbf{A} = [A_{-H}, \dots, A_H], \mathbf{B} = [B_{-H}, \dots, B_H]$ can be expressed as a convolution in Fourier space,

$$\mathcal{F}\{a \cdot b\} = \mathbf{A} * \mathbf{B}. \quad (10)$$

Herein, \mathcal{F} indicates the Fourier Transform and $*$ denotes convolution. Note that powers of a Fourier series can be calculated by recursive multiplication.

The *integration* of a truncated Fourier series in the time interval τ^- to τ^+ can be expressed as follows (see Appendix A):

$$\int_{\tau^-}^{\tau^+} a(\tau) e^{-in\tau} d\tau = (\tau^+ - \tau^-) A_n + \sum_{m=-H, m \neq n}^H \frac{e^{i(m-n)\tau^+} - e^{i(m-n)\tau^-}}{i(m-n)} A_m. \quad (11)$$

This equation can be applied to the evaluation of the integrals in Eq. (5).

There are efficient as well as robust numerical methods for the *calculation of the roots* of a truncated Fourier series, see e.g. [12]. Most of these methods simply compute the roots of the associated complex polynomial in $z = e^{i\tau}$. Such methods are available in many computational software frameworks like Matlab.

It is important to note that the harmonic order is increased by the convolution in Eq. (10), i. e. when products or powers of a Fourier series are generated. It is therefore proposed to truncate the Fourier series of the nonlinear function \mathbf{F}_n

to the original order H in Eq. (4) so that the resulting number of equations is equal to the number of unknowns.

2.6. On the numerical performance and accuracy of the proposed method

In all numerical studies of the piecewise polynomial systems presented in Section 3, the computational bottleneck was observed to be the root finding of the complex polynomials involved in the calculation of the state transition time instants. State-of-the art polynomial root finding algorithms are based on the computation of the eigenvalues of a so called companion matrix, for which the computational complexity increases approximately with the number of harmonics cubed $\mathcal{O}(H^3)$. The interested reader is referred to [12] for a detailed analysis of the computational cost for this operation.

In contrast to the root finding operation, carrying out time-domain integration, differentiation and multiplication by means of summation and matrix multiplication according to the derived closed-form expressions in Subsection 2.5 is comparatively efficient. This has some noteworthy implications for the analytical calculations of the gradients: The evaluation of first and second order derivatives represents an efficient post-processing step, since their calculation only involves comparatively cheap vector and matrix multiplications, as indicated in Subsection 2.4.

It should be remarked that the accuracy of the proposed method, particularly regarding the gradients, relies on the direct calculation of the state transitions. The conventional AFT scheme is characterized by an inherent discretization error. This causes a severe limitation for the achievable accuracy. In this context, it is interesting to note that in a piecewise linear system, the second-order derivatives essentially result from the sensitivities of the transition time instants, which can be easily verified from Eq. (9). As these sensitivities are not captured by the AFT scheme, the second-order sensitivities would be identical to zero in this case. This emphasizes the superiority of the proposed method with respect to the AFT scheme regarding accurate sensitivity analysis.

3. Numerical examples

We have implemented the methodology proposed in Section 2 in a computational framework in the Matlab software environment. We used an object-oriented software architecture to exploit operator overloading capabilities. For example, we defined a Fourier series class that implements the required operations add/subtract, multiply, integrate and compute roots. Moreover, we developed and used an Automatic Differentiation class similar to the one described in [13, 14] to carry out the analytical sensitivity analysis up to second order. A database of state formulations was created that includes the nonlinearities presented in this section.

The numerical examples in this study comprise structural dynamical systems. Application of the proposed methodology to fields other than structural dynamics, e. g. electrical networks, is considered straight-forward but beyond the scope of this study. For structural dynamical systems, the vectors \mathbf{y} , \mathbf{f} can be written as follows:

$$\mathbf{y} = \begin{bmatrix} \mathbf{x} \\ \dot{\mathbf{x}} \end{bmatrix}, \quad \mathbf{f} = \begin{bmatrix} \dot{\mathbf{x}} \\ -\mathbf{M}^{-1} \left(\mathbf{D}\dot{\mathbf{x}} + \mathbf{K}\mathbf{x} + \mathbf{f}_e(t) + \tilde{\mathbf{f}}(\mathbf{x}, \dot{\mathbf{x}}) \right) \end{bmatrix}. \quad (12)$$

Herein, \mathbf{M} , \mathbf{D} , \mathbf{K} are structural mass, damping and stiffness matrices, \mathbf{x} is the vector of generalized displacements, \mathbf{f}_e , $\tilde{\mathbf{f}}$ are generalized excitation and nonlinear forces.

The numerical examples can be categorized in two groups. In the examples in Subsections 3.1-3.4 a 2-Degree-of-freedom (DOF) system with an attached single nonlinear element \tilde{f} is considered, see Fig. 3. The example for Subsection 3.5 is a cantilevered beam with contact constraints and will be described later. It should be noted that the example systems with a small number of DOFs were considered for clarity reasons. The methodology proposed in this paper can generally be applied to systems with arbitrary number of DOFs, including large-scale Finite Element Models.

For the 2-DOF system, the structural matrices and the nonlinear force vector

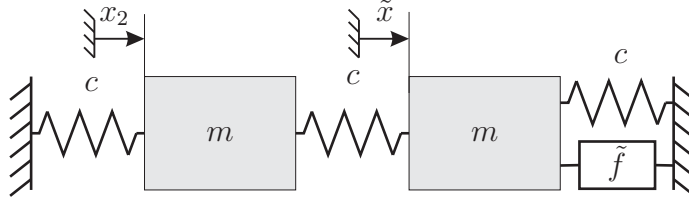


Figure 3: 2-DOF system with nonlinear element

have the following form:

$$\mathbf{M} = \begin{bmatrix} 1 & 0 \\ 0 & 1 \end{bmatrix}, \quad \mathbf{D} = \mathbf{0}, \quad \mathbf{K} = \begin{bmatrix} 2 & -1 \\ -1 & 2 \end{bmatrix}, \quad \tilde{\mathbf{f}} = \begin{bmatrix} \tilde{f} \\ 0 \end{bmatrix}.$$

The corresponding vector of generalized coordinates is $\mathbf{x}^T = [\tilde{x} \quad x_2]$, where \tilde{x} denotes the nonlinear DOF.

3.1. 2-DOF system with cubic spring

For a first demonstration of the methodology, a cubic spring nonlinearity is considered. The nonlinearity can be described by a single state without transition conditions and no internal variables. In the notation introduced in Eq. (2), the state definition reads as listed in Tab. 1.

Table 1: State definition of a system with cubic spring

state 1	
\tilde{f}	$0.5\tilde{x}^3$
g	(-)
v	(-)

This example emphasizes once again that purely polynomial, i. e. smooth nonlinearities are a special case of the piecewise polynomial class treated in this study.

The 2-DOF system is investigated in autonomous configuration. The proposed method was used for the calculation of the nonlinear normal modes. Great convergence behavior was ascertained.

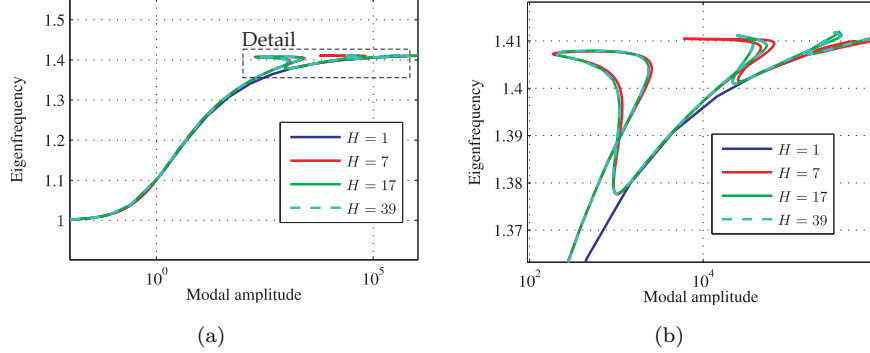


Figure 4: Frequency-Energy-Plot of a 2-DOF system with cubic spring ((a) overview, (b) detail)

A thorough study of the nonlinear normal modes of this system can be found in KERSCHEN ET AL. [15] and shall not be repeated here. Instead, only the so called Frequency-Energy-Plot (FEP) of the first nonlinear mode is depicted in Figs. 4a-4b. Throughout this study, amplitude and frequency axes in the figures are scaled by their values for the linear case. The eigenfrequency increases with the modal amplitude due to the stiffening effect of the cubic spring. For large amplitudes, the energy localizes in the left mass in Fig. 3. The system exhibits several internal resonances in the considered modal amplitude range [15], causing so called tongues in the FEP, see Fig. 4b. Apparently several harmonics are required to accurately predict the nonlinear modal interactions.

3.2. 2-DOF system with piecewise polynomial spring

Again, the 2-DOF system is considered, however, the cubic spring is now replaced by a piecewise polynomial spring. The force-displacement characteristic is given by the function depicted in Fig. 5a. The nonlinearity was defined by introducing three states, each with a polynomial force \tilde{f} as listed in Tab. 2. As it was shown in Section 2.5, the High-order Harmonic Balance residual equations can be formulated analytically for this class of systems by the new technique proposed in this paper.

The central part of the characteristic is linear with negative slope. The two

Table 2: State definition of a system with piecewise polynomial spring

	state 1	state 2	state 3
\tilde{f}	$-(\tilde{x} - 1)^2 + 1$	$-(\tilde{x} - 2)$	$(\tilde{x} - 3)^2 - 1$
g	$g_{12} = \tilde{x} - 1$	$g_{21} = g_{12}, g_{23} = g_{32}$	$g_{32} = \tilde{x} - 3$
v	(-)	(-)	(-)

neighboring states have a quadratic force-displacement characteristic. Note that the piecewise polynomial spring is conservative with a unique force-displacement relationship. Hence, the state formulation does not require any internal variables.

A harmonic force excitation at the linear mass in a frequency range close to the first eigenfrequency is imposed. The forced response function was calculating using the proposed method and is illustrated in Fig. 5b. Overhanging branches occur in the forced response characteristic: For moderate vibration amplitudes, i. e. for small vibrations around the equilibrium point $\tilde{x} = 0$, the system exhibits softening behavior and the amplitude-frequency curve is bent to the left. The effective stiffness decreases with increasing amplitude due to negative slope in the force-displacement characteristic. For larger vibration amplitudes, the effective stiffness increases due to the quadratic branches, resulting in a stiffening

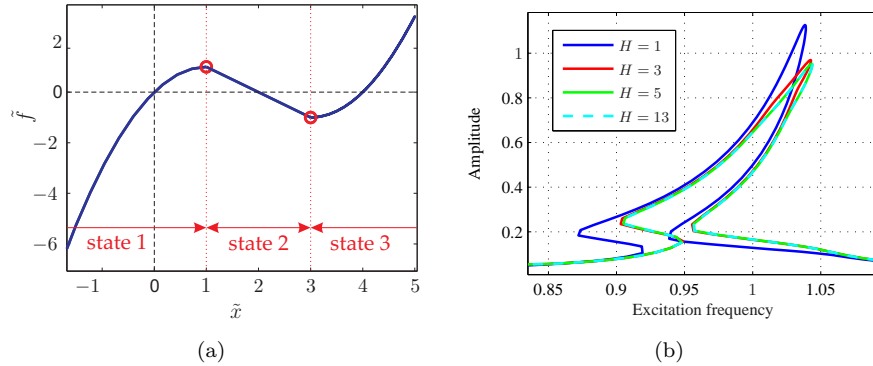


Figure 5: Characteristics of a 2-DOF system with piecewise polynomial spring ((a) force-displacement relationship, (b) forced response function)

behavior and the amplitude-frequency curve is bent to the right. Apparently, several harmonics have to be considered in the harmonic expansion to accurately predict the dynamic behavior of the system.

3.3. 2-DOF system with elastic Coulomb friction element

An elastic Coulomb friction or Masing element [16] is attached to the 2-DOF system in Fig. 3. Tangential stiffness k_t and friction force limit F_R characterize this nonlinearity. The nonlinearity can assume two states: Stick (state 1) and slip (state 2), see Tab. 3.

Table 3: State definition of a system with elastic Coulomb friction element

	state 1	state 2
\tilde{f}	$k_t(\tilde{x} - v_1)$	$v_2 F_R$
g	$g_{12} = \tilde{f}^2 - (F_R)^2$	$g_{21} = \dot{\tilde{x}}$
v	$v_1 = \tilde{x}(\tau_j^-) - \frac{\tilde{f}(\tau_j^-)}{k_t}$	$v_2 = \text{sgn} \tilde{f}(\tau_j^-)$

If the elastic friction force reaches its limit value F_R , i. e. $g_{12} = 0$, a stick-to-slip transition occurs. If a reversal point is reached ($\dot{\tilde{x}} = g_{21} = 0$), a stick phase is initiated. Internal variables for the elastic Coulomb element are the Coulomb slider position v_1 and the slip direction v_2 .

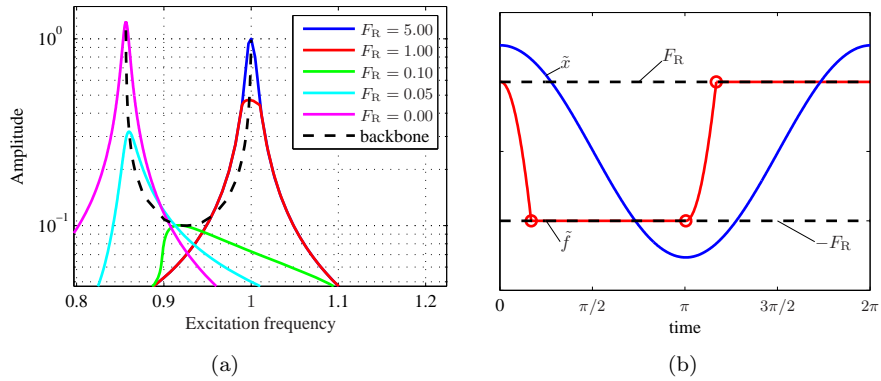


Figure 6: Forced response of a system with elastic Coulomb nonlinearity ((a) forced response functions for different values of the normal load, (b) typical time history)

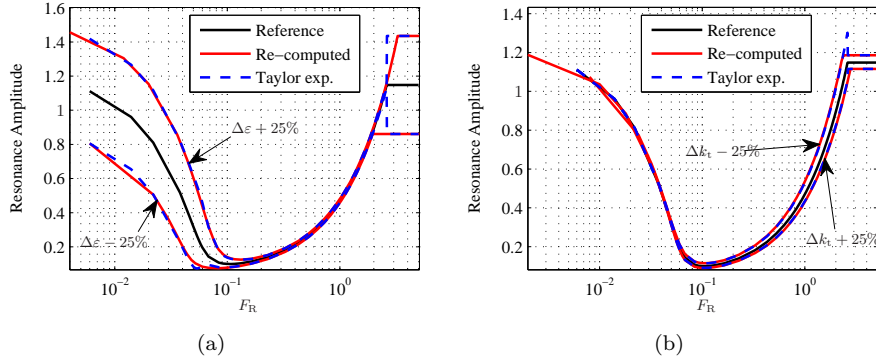


Figure 7: Resonance amplitude as a function of the normal load ((a) variation of the excitation level ε , (b) variation of the tangential stiffness k_t)

Again, a harmonic force excitation is imposed at the linear mass. In Fig. 6a, the forced response function in the vicinity of the eigenfrequency of the first mode is depicted for different values of the friction force limit F_R . A tangential stiffness value of $k_t = 0.35$ was specified. For large values of F_R , the Coulomb element is fully stuck so that the hysteresis degenerates to a line and no damping effect is introduced by the friction element. For vanishing values of F_R , the slider can slip freely so that the hysteresis is flat and again there is no friction damping effect. In between these extreme cases, a significant amplitude reduction due to friction damping can be achieved. Moreover, the resonance frequency increases as the value of F_R increases due to the coupling effect of the friction element. The backbone curve that connects the maxima of the forced response functions was directly calculated by applying the strategy described in [17] to the methodology proposed in this paper. A typical time history of both displacement \tilde{x} and nonlinear force \tilde{f} is illustrated in Fig. 6b. Owing to the moderate value of k_t , the response remains essentially harmonic. The transitions between stick and slip state can be well-observed from the time history of the force in Fig. 6b. The suitability of the analytically formulated sensitivities is now investigated. To this end, the resonance amplitude of the first mode is depicted as a direct function of F_R in Figs. 7a-7b. These so called optimization curves are often

used for design purposes, see e.g. [18, 19, 20]. In addition to the nominal parameter set, the optimization curve is also illustrated for slightly smaller and larger ($\pm 25\%$) excitation level and tangential stiffness values. The results were obtained by second-order Taylor expansion about the reference solution (Taylor exp.). For comparison, the optimization curves were also computed directly at the new parameter point (Re-computed). The results agree well in a wide range of the F_R value. However, the Taylor expansion fails in predicting the fully stuck configuration, i.e. for very high F_R values. As it was also reported in [21, 17], it is not possible to accurately predict the dynamic behavior beyond the point where the order or number of states change.

3.4. 2-DOF system with superelastic shape memory alloy

The hysteresis effect of superelastic shape memory alloys (SMA) can be employed for damping of mechanical structures. A sophisticated modeling approach would involve constitutive as well as thermodynamical aspects, see e.g. [22]. This is, however, regarded as beyond the scope of this study and a simplified rheological piecewise linear model [2] shall be considered instead. The associated hysteresis can be described by five distinct states as illustrated in Fig. 8 and listed in Tab. 4. The system features a purely elastic state (1). The forward and reverse transformation between austenite and martensite phase is described by the states (2) and (4). Beyond a certain displacement, a linear onset (3) is used to describe the superelastic behavior. Depending on the displacement evolution in time, an intermediate state (5) can also be reached. Note that the point symmetry of the hysteresis is exploited in the state definition in Tab. 4.

The SMA-type nonlinearity was also applied to the 2-DOF system in Fig. 3. The Nonlinear Modal Analysis technique proposed in [23, 24] was employed in conjunction with the formulations of the nonlinearities proposed in this study. Eigenfrequency and the modal damping ratio were computed with respect to the modal amplitude of the first mode. The results are depicted in Figs. 9a-9b. For small vibration amplitudes, the system always remains in state 1, i.e. the

Table 4: State definition of a system with superelastic shape memory alloy

	state 1	state 2	state 3
\tilde{f}	$k\tilde{x}$	$v_2(F_0 + F_R)$	$k(\tilde{x} - v_3a)$
g	$g_{12} = \tilde{f}^2 - (F_0 + F_R)^2$	$g_{23} = kv_2\tilde{x} - ka - F_0 - F_R,$ $g_{25} = \dot{\tilde{x}}$	$g_{34} = \tilde{f} - v_3(F_0 - F_R)$
v	$(-)$	$v_2 = \text{sgn } \tilde{x}(\tau_j^-)$	$v_3 = v_2$

	state 4	state 5
\tilde{f}	$v_4(F_0 - F_R)$	$k(\tilde{x} - v_5)$
g	$g_{41} = kv_3\tilde{x} - F_0 + F_R,$ $g_{45} = \dot{\tilde{x}}$	$g_{52} = \tilde{f}^2 - (F_0 + F_R)^2,$ $g_{54} = \tilde{f}^2 - (F_0 - F_R)^2$
v	$v_4 = v_2$	$v_5 = \tilde{x}(\tau_j^-) - \frac{\tilde{f}(\tau_j^-)}{k_t}$

damping vanishes and the eigenfrequency is constant. For moderate vibration amplitudes, the phase transformation occurs to a certain extent so that the damping value increases and the eigenfrequency is reduced due to the softening effect. For large vibration amplitudes, the effect of the hysteresis cycles becomes smaller again so that eigenfrequency and damping value asymptotically

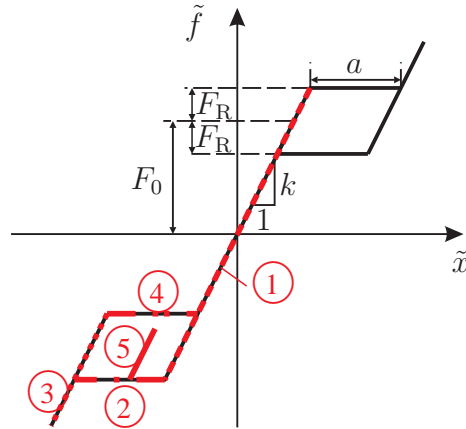


Figure 8: Approximated hysteresis of a superelastic shape memory alloy

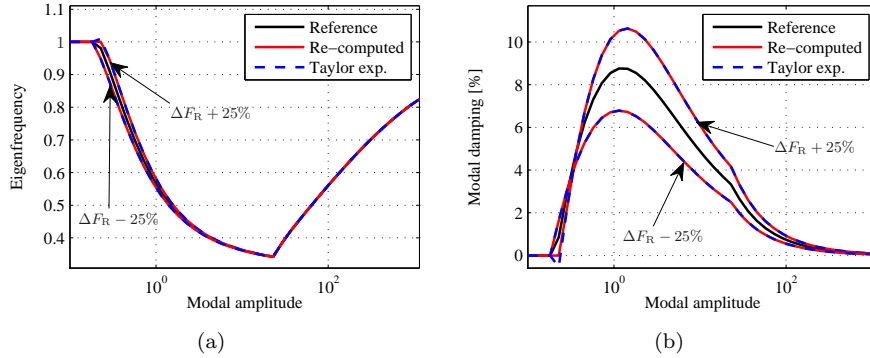


Figure 9: Modal properties of a 2-DOF system with superelastic shape memory alloy ((a) eigenfrequency, (b) modal damping)

approach their linearized values again.

As in the previous example, the sensitivities of the nonlinear dynamic analysis results have been computed to formulate a second-order Taylor series in the system parameters. Using the sensitivity results, the modal properties have been expanded with respect to the parameter F_R , cf. Figs. 9a-9b, for $\pm 25\%$ deviation from the nominal value. The results agree well with the re-computed results.

3.5. Beam with friction and unilateral contact

As a final example, a clamped beam with combined friction and unilateral contact was investigated. The system is depicted in Fig. 10. A finite element code was used to mesh the geometry and derive the structural matrices of the cantilevered beam for the initial configuration. The finite element model comprised 10,098 DOFs. A single node-to-ground contact element was attached to the free end as depicted in Fig. 10. In contrast to the example in Subsection 3.3,

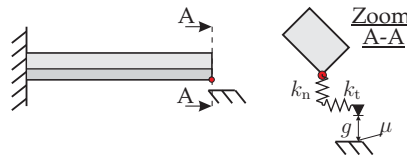


Figure 10: Cantilevered beam with friction and unilateral contact at its free end

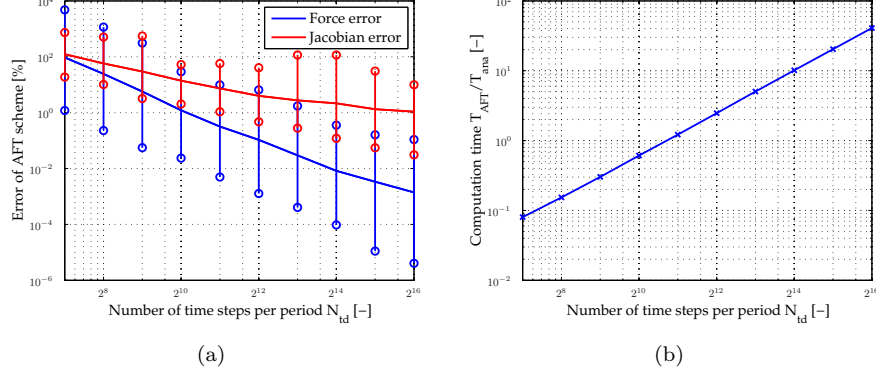


Figure 11: Comparison of Alternating-Frequency-Time scheme with proposed method ((a) accuracy of function and derivative, (b) computational effort)

the contact model additionally accounts for the variation of the normal load and possible lift-off. The contact nonlinearity can thus assume three distinct states as listed in Tab. 5: Separation (state 1), stick (state 2), slip (state 3). System parameters are tangential stiffness k_t , friction coefficient μ , normal stiffness k_n and normal gap g .

Table 5: State definition of a system with friction and unilateral contact

	state 1	state 2	state 3
$\tilde{\mathbf{f}}$	$\begin{bmatrix} 0 \\ 0 \end{bmatrix}$	$\begin{bmatrix} k_n (\tilde{x}[1] + g) \\ k_t (\tilde{x}[2] - v_2) \end{bmatrix}$	$\begin{bmatrix} k_n (\tilde{x}[1] + g) \\ v_3 \mu k_n (\tilde{x}[1] + g) \end{bmatrix}$
g	$g_{12} = \tilde{x}[1] + g$ if $k_n \dot{\tilde{x}}[1] > k_t \dot{\tilde{x}}[2]$, $g_{13} = \tilde{x}[1] + g$ if $k_n \dot{\tilde{x}}[1] \leq k_t \dot{\tilde{x}}[2]$	$g_{21} = \tilde{x}[1] + g$, $g_{23} = \left(\tilde{f}[2] \right)^2 - \left(\mu \tilde{f}[1] \right)^2$	$g_{31} = g_{21}$, $g_{32} = \dot{\tilde{f}}[2] - k_t \dot{\tilde{x}}[2]$
v	(-)	$v_2 = \tilde{x}[2](\tau_j^-) - \frac{\tilde{f}[2](\tau_j^-)}{k_t}$	$v_3 = \text{sgn } \tilde{f}[2](\tau_j^-)$

For this particular example, a comparison with the conventional AFT scheme was performed in terms of accuracy and computational effort, cf. Figs. 11a-11b. Only the nonlinear force calculation is considered for the comparison. Random vectors of complex displacement amplitudes was generated. A number of 1,000 random vectors was large enough to obtain convergence of the performance

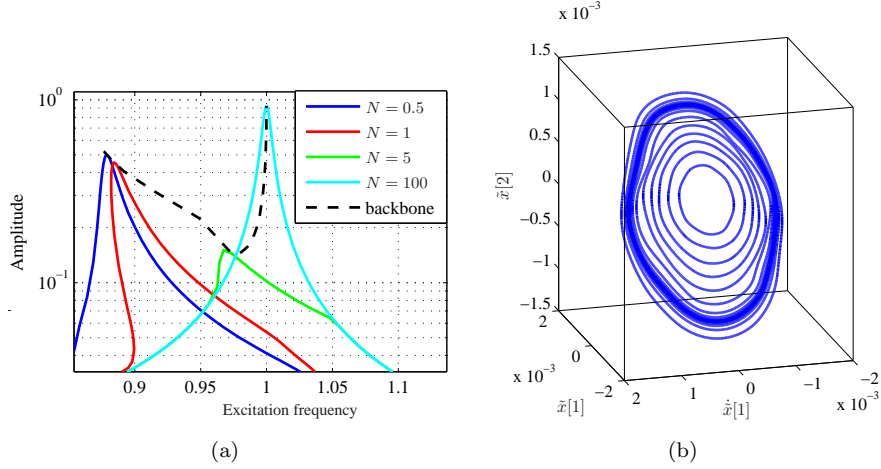


Figure 12: Forced response of a beam with friction and unilateral contact ((a) forced response functions for different values of the normal load, (b) orbits along the backbone curve)

statistics. Seven harmonics have been considered in the analysis. In Fig. 11a, the mean, minimum and maximum error of the force and the Jacobian are depicted with respect to the number of time samples N_{td} per period used in the AFT scheme. The accuracy of the AFT scheme can be increased by increasing the number of time steps. A larger number of time steps yields a better accuracy, but also a higher computational effort. The computational effort T_{AFT} essentially increases linearly with the number of time steps. The effort quickly exceeds the one required for the proposed method (T_{ana}), cf. Fig. 11b. It has to be remarked that only the nonlinear force is considered in the performance comparison. It is expected that the resulting error in the predicted response is less significant than that of the force or the Jacobian.

A harmonic force excitation was imposed at the center of the free end in a frequency range near the second bending eigenfrequency. The forced response for varied normal preload $N = -g/k_n$ is depicted in Fig. 12a along with the backbone curve. The results are generally similar to the ones presented in Subsection 3.3. Again, it can be ascertained that there exists an optimum normal preload that minimizes the resonance amplitude. For smaller preload values,

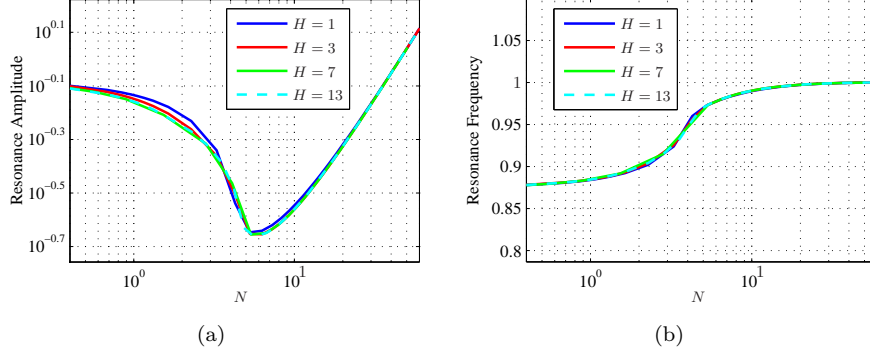


Figure 13: Resonance properties for different orders of the harmonic balance approach ((a) resonance amplitude, (b) resonance frequency)

the contact node may lift off during one period of oscillation. This causes a softening effect, leading to overhanging branches in the forced response characteristic. In Fig. 12b, some periodic orbits corresponding to points on the backbone curve are illustrated in a three-dimensional section through the phase space. According to expectations, a multiharmonic character can be ascertained from the response. In particular, the static component of the displacement is varying with the vibration amplitude.

In Figs. 13a-13b, resonance amplitude and frequency are depicted as a direct function of the normal preload N . Several harmonics are required to achieve asymptotic convergence of the resonance properties. This particularly holds for smaller values of N i. e. when the oscillation of the normal load and partial separation gain influence on the dynamics of the system.

4. Conclusions

A method was proposed that allows for an analytical formulation of the high-order Harmonic Balance Method for the dynamic analysis of systems with distinct states. The method can be applied to generic nonlinearities that can be described by piecewise polynomial functions and state transition conditions. The methodology not only facilitates the computation of the periodic solution

but also provides accurate sensitivity data of the solution to arbitrary system parameters that can be used e. g. for design studies. It was shown that the approach can be superior to the conventional Alternating-Frequency-Time scheme in terms of accuracy and computational efficiency, in particular if the sensitivities of the transition time instants between the states are of interest.

The method was applied to several structural dynamical systems with conservative and dissipative nonlinearities in externally excited and autonomous configurations. Generally good performance and robustness of the numerical method were observed.

Possible future work includes a comparison of the method to the Harmonic Balance formulation of the Asymptotic Numerical Method, as introduced in [9], and the application to other engineering fields such as electrical switching networks.

Appendix A. Definite integral of a truncated Fourier series

A truncated Fourier series $a(\tau)$ is considered,

$$a(\tau) = \sum_{m=-H}^H A_m e^{im\tau}. \quad (\text{A.1})$$

Substituting this definition into Eq. (11) yields

$$\int_{\tau^-}^{\tau^+} a(\tau) e^{-in\tau} d\tau = \int_{\tau^-}^{\tau^+} \sum_{m=-H}^H A_m e^{im\tau} e^{-in\tau} d\tau = \sum_{m=-H}^H A_m \int_{\tau^-}^{\tau^+} e^{i(m-n)\tau} d\tau. \quad (\text{A.2})$$

The indefinite integral of the integral in the last part of Eq. (A.2) can be expressed as

$$\int e^{i(m-n)\tau} d\tau = \begin{cases} \tau & m = n \\ \frac{e^{i(m-n)\tau}}{i(m-n)} & m \neq n \end{cases}. \quad (\text{A.3})$$

The case $m = n$ thus has to be treated separately. For convenience, the sum in Eq. (A.2) is therefore split up. Substituting Eq. (A.3) into Eq. (A.2) finally gives

$$\begin{aligned}
\int_{\tau^-}^{\tau^+} a(\tau) e^{-in\tau} d\tau &= \left[A_n \tau + \sum_{m=-H, m \neq n}^H A_m \frac{e^{i(m-n)\tau}}{i(m-n)} \right]_{\tau^-}^{\tau^+} \\
&= (\tau^+ - \tau^-) A_n + \sum_{m=-H, m \neq n}^H \frac{e^{i(m-n)\tau^+} - e^{i(m-n)\tau^-}}{i(m-n)} A_m.
\end{aligned}
\tag{A.4}$$

References

- [1] K. L. Johnson, Contact mechanics, repr. Edition, Cambridge University Press, Cambridge, 1989.
- [2] I. Schmidt, Untersuchungen zur Dämpfungskapazität superelastischer Nickel-Titan-Formgedächtnislegierungen, Ph.D. thesis, Universität der Bundeswehr Hamburg, Hamburg (01.01.2004).
- [3] M. Urabe, Galerkin's procedure for nonlinear periodic systems, Archive for Rational Mechanics and Analysis 20 (2) (1965) 120–152.
- [4] A. H. Nayfeh, D. T. Mook, Nonlinear oscillations, John Wiley & Sons, New York 1979.
- [5] L. Salles, L. Blanc, F. Thouverez, A. M. Gousskov, P. Jean, Dual Time Stepping Algorithms With the High Order Harmonic Balance Method for Contact Interfaces With Fretting-Wear, Paper GT2011-46488, Proc. of GT2011, ASME Turbo Expo 2011: Advancing Clean and Efficient Turbine Technology, June 7-10, Vancouver, Canada (2011).

- [6] A. Gopinath, A. Jameson, Time spectral method for periodic unsteady computations over two-and three-dimensional bodies, AIAA Paper 1220 (2005) 10–13.
- [7] T. M. Cameron, J. H. Griffin, An Alternating Frequency/Time Domain Method for Calculating the Steady-State Response of Nonlinear Dynamic Systems, *Journal of Applied Mechanics* 56 (1) (1989) 149–154.
- [8] J. Guillen, C. Pierre, An Efficient, Hybrid, Frequency-Time Domain Method for the Dynamics of Large-Scale Dry-Friction Damped Structural Systems, *Proc. of the IUTAM Symposium held in Munich, Germany, August 3-7 (1998)*.
- [9] B. Cochelin, C. Vergez, A high order purely frequency-based harmonic balance formulation for continuation of periodic solutions, *Journal of Sound and Vibration* 324 (1–2) (2009) 243–262.
- [10] E. P. Petrov, D. J. Ewins, Analytical Formulation of Friction Interface Elements for Analysis of Nonlinear Multi-Harmonic Vibrations of Bladed Disks, *Journal of Turbomachinery* 125 (2) (2003) 364–371.
- [11] R. Seydel, *Practical bifurcation and stability analysis: from equilibrium to chaos*, Springer, 1994.
- [12] J. Boyd, Computing the zeros, maxima and inflection points of Chebyshev, Legendre and Fourier series: solving transcendental equations by spectral interpolation and polynomial rootfinding, *Journal of Engineering Mathematics* 56 (3) (2006) 203–219.
- [13] S. A. Forth, An efficient overloaded implementation of forward mode automatic differentiation in MATLAB, *ACM Trans. Math. Softw* 32 (2) (2006) 195–222.
- [14] R. Neidinger, Introduction to Automatic Differentiation and MATLAB Object-Oriented Programming, *SIAM Review* 52 (3) (2010) 545–563.

- [15] G. Kerschen, M. Peeters, J. C. Golinval, A. F. Vakakis, Nonlinear normal modes, Part I: A useful framework for the structural dynamicist: Special Issue: Non-linear Structural Dynamics, *Mechanical Systems and Signal Processing* 23 (1) (2009) 170–194.
- [16] G. Masing, Zur Heynschen Theorie der Verfestigung der Metalle durch verborgene elastische Spannungen, *Wissenschaftliche Veröffentlichungen aus dem Siemens-Konzern* 3 (1) (1923/24) 231–239.
- [17] M. Krack, L. Panning-von Scheidt, J. Wallaschek, C. Siewert, A. Hartung, Robust Design of Friction Interfaces of Bladed Disks With Respect to Parameter Uncertainties, Paper GT2012-68578, *Proc. of ASME Turbo Expo 2012*, June 11-15, Copenhagen, Denmark (2012).
- [18] M. Berthillier, C. Dupont, R. Mondal, J. J. Barrau, Blades Forced Response Analysis with Friction Dampers, *Journal of Vibration and Acoustics* 120 (2) (1998) 468–474.
- [19] E. P. Petrov, Direct Parametric Analysis of Resonance Regimes for Non-linear Vibrations of Bladed Discs, Paper GT2006-90147, *Proc. of GT2006, ASME Turbo Expo 2006: Power for Land, Sea and Air*, May 8-11, Barcelona, Spain (2006).
- [20] M. Krack, A. Herzog, L. Panning-von Scheidt, J. Wallaschek, C. Siewert, A. Hartung, Multiharmonic Analysis and Design of Shroud Friction Joints of Bladed Disks Subject to Microslip, Paper DETC2012-70184, *Proc. of ASME 2012 International Design Engineering Technical Conferences & Computers and Information in Engineering Conference (IDETC/CIE 2012)*, August 12-15, Chicago, USA (2012).
- [21] R. D. Braun, I. M. Kroo, P. J. Gage, Post-optimality analysis in aerospace vehicle design, *AIAA Paper* (1993) 93–3932.
- [22] D. Bernardini, F. Vestroni, Non-isothermal oscillations of pseudoelastic

devices, *International Journal of Non-Linear Mechanics* 38 (9) (2003) 1297–1313.

[23] D. Laxalde, F. Thouverez, Complex non-linear modal analysis for mechanical systems Application to turbomachinery bladings with friction interfaces, *Journal of Sound and Vibration* 322 (4-5) (2009) 1009–1025.

[24] M. Krack, L. Panning-von Scheidt, J. Wallaschek, A. Hartung, C. Siewert, Reduced Order Modeling Based on Complex Nonlinear Modal Analysis and its Application to Bladed Disks With Shroud Contact, Paper GT2013-94560, Proc. of ASME Turbo Expo 2013, June 3-7, San Antonio, Texas, USA (2013).